MICRO-SCALE STUDY OF RESIDUAL STRESSES IN CR$_2$O$_3$ COATINGS SPRAYED BY APS

Franck Decroos[a,*], Cécile Langlade[a], Eric Bourillot[a], Geoffrey Darut[a], Manuel Francois[b]

[a] *Université de Bourgogne Franche-Comté, Laboratoire Interdisciplinaire Carnot de Bourgogne, Site de Sevenans, 90 010 Belfort cedex, France*

[b] *Université de Technologie de Troyes, Charles Delaunay Institute, Life Assement of Structures, Materials and Integrated Systems, 12 rue Marie Curie, 10 004 Troyes CEDEX, France*

* corresponding author: franck.decroos@utbm.fr

Abstract. Whichever the application field, every material forming process generates residual stresses on the surface. While they are likely to enhance the aimed properties of the final mechanical part, these stresses may also drastically reduce them and result in early failures. Therefore, understanding the residual stress state remains a major challenge when coating complex parts, especially as most characterization methods at the microscopic scale involve specific sample preparation procedures which may affect the residual stresses field. This work investigates the residual stress state that exists in chromium oxide coatings deposited via Atmospheric Plasma Spray (APS), using two pioneering techniques featuring high spatial resolution: Scanning Microwave Microscopy and Raman Micro-Spectroscopy. The first technique combines the measurement of microwave electromagnetic capacities of a Vector Network Analyzer with the subnanometric resolution of an Atomic Force Microscope: it thus enables performing depth investigations at very accurately defined positions of the probe on the surface. The second technique relies on the principle of photons inelastic scattering and involves a laser beam aiming at the material sample: it allows a fine characterization of the microstructure as well as defects and stresses detection via molecular vibratory signatures. The investigation scale is limited here to a few cubic micrometers. Due to the highly localized scales of our investigations, which also depend on the device, the objective of our procedure required that the comparison should be made not on individual points but on definite mapped areas, every spot being analyzed and post-treated one after another, with optimum measuring parameters. Results have been correlated with XRD measurements to cross-check the average amount of stress observed over a wider area.

Keywords: Coatings, chromium oxides, Raman Micro-Spectroscopy, residual stress, scanning microwave microscopy.

1. Introduction

1.1. Residual stresses in thermal spray coatings

It is today widely-known that residual stresses (RS) have significant implications in both the preparation and the performance of thermally sprayed coatings. On one hand, tensile stresses are generally recognized to reduce service lifetime, weaken interfacial adhesion, and sometimes cause early delamination when they exceed the elastic limit of the material. On the other hand, compressive stresses are most often associated with better performance and fewer micro-cracks, which are known to enhance corrosion resistance during service [1–3]. Thus, assessing the RS field of a coating is a major concern to optimize spraying parameters and match technical specifications. By doing so, a more accurate prediction of the in-service behavior of the coating is possible. Important properties of RS are magnitude, sign, and even more specifically their superficial distribution.

1.2. Origins of residual stresses

Thermal spray processes involve various stress generating phenomena. When dealing with ceramic coatings deposited via Atmospheric Plasma Spray (APS), the most significant are the following. The first one is the effect of quenching, when the shrinkage of individual splats leads to local stress generation as the coating is cooling from its melting temperature to the substrate temperature. Simultaneously, stress-relaxation mechanisms such as interfacial sliding and extensive microcracking may occur, microcracking being very common in ceramic materials [4–7]. The second phenomenon is due to the mismatch between the Coefficients of Thermal Expansion (CTE) of the coating and the substrate [1], [8]. A further effect lies in the transient injection of heat fluxes into the substrate, hence generating important thermal gradients which cause differential thermal expansion at different depths as well as changes to the local misfit strains [1]. This point is important in our study as the depth of investigation varies for the two tech-

niques employed. Macro stresses (type 1 RS) and joint stresses (type 2 RS) are worth investigating in our case in consideration of the engineering objective [9].

1.3. Purpose of the work

In practice, the superimposition of the various phenomena mentioned above generates a complex RS field and makes the in-service behavior of APS coatings difficult to predict. Therefore, the objective of this work is to combine new investigation methods for local determination of the RS field, targeting the two kinds of stress mentioned above. The first method is the Raman micro-spectroscopy, which is increasingly used in this field [9–14]. This technology enables fast micro-scale measurements on Raman-active materials such as oxides [9, 10].Here, lattice bondings will be submitted to vibration through the inelastic photon scattering phenomenon using a low power laser emission. Hence, all molecules are characterized by a unique spectrum. The fingerprint spectrum and behavior law of Raman peaks regarding stress are today known for common types of materials including Cr_2O_3 [11, 12]. The second method is a custom Scanning Microwave Microscope (SMM) performing nano or micro-scale measurements, here used for the first time on ceramics [13]. Hence, the study also aims to calibrate this new instrument using Raman spectrometer as reference. SMM features two advantages: a 20 nm diameter area of investigation at surface, and the data collection at different depths underneath this small area. Moreover, this is a non-destructive investigation method. Indeed, RS measurement is assessed while measuring the signal amplitude, which will vary with changes in lattice organization of the investigated material. A more complete theory is available in "Experimental Section" of Aybeke, EN and al. paper [14]. This in-depth technique represents a significant change in stress investigation, especially when dealing with ceramic coatings. Finally, X-Ray Diffraction (XRD) measurements based on the $\sin^2(\psi)$ method will be correlated to the previous results. XRD stands for the reference in our field [1, 9]. To do so, mappings have been performed with both more local devices in order to be compared to XRD wider area. Raman spectrometer and top surface SMM mappings results can be expected to exhibit similar tendencies as both investigate changes in lattice organization.

These investigation technologies have been applied on Cr_2O_3 coatings performed by APS: the spraying temperature was chosen as the varying parameter to elaborate different residual stress fields.

2. Methods

2.1. Materials and coating deposition

Chromium oxide coatings were deposited via APS upon a 30 mm × 30 mm × 5 mm steel substrate using commercially available chromium oxide powder from Saint-Gobain. Before deposition, substrates were sandblasted so that the Ra was superior to 4 µm, then they were cleaned in ethanol.

In order to investigate differences between RS fields, this paper deals with two samples:

(1.) Ref1 which was performed using optimized parameters and procedure for thermal barriers coating applications at a depositing temperature of 200 °C. Thickness is 200 µm.

(2.) HT2 which only differs from the previous one by its depositing temperature that was about 450 °C. Thickness is 400 µm.

The main spraying parameters are listed in Table 1. Measurements were conducted on as-deposited coatings.

Spraying parameters	Value
Current intensity (A)	650
Ar/H2 ratio	40/13
Gas flow rate (L.min-1)	3
Spraying distance (mm)	110

Table 1. Main spraying parameters

2.2. Scanning Microwave Microscopy

The used Scanning Microwave Microscope is an original device from Agilent which has been widely customized since it was bought. It is basically made out of two parts as showed in Figure 1.
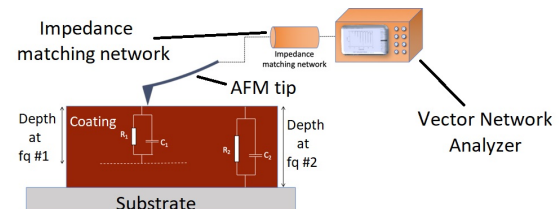

Figure 1. Scanning Microwave Microscope

The first one is an Atomic Force Microscope (AFM), equipped with a probe which will be used as an antenna to emit as well as to receive the microwave signal. To do so, being in the near field becomes a necessary condition in order to emit a directive signal. Thus, the tip of the probe was put directly in contact with the sample surface. Besides, the design of the tip also guarantees the high resolution of the measurement as its diameter is no more than 20 nanometers. The second part of the device is a Vector Network Analyzer (VNA). At first, this VNA generates a wave train of a sinusoidal microwave signal at a very low power. Then, it compares the generated signal to the one which is reflected. In short, VNA outputs the S11 reflection coefficient.

As a matter of fact, generating a wave train of various frequencies enables in-depth investigation of
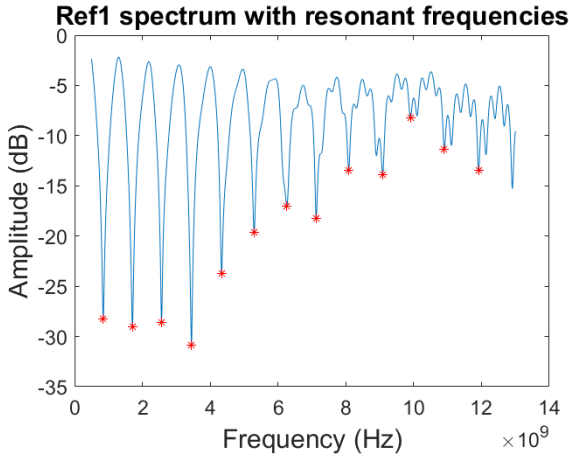
FIGURE 2. A typical microwave signal

FIGURE 3. Edge effects in SMM

a material. Hence, a finite number of depths can be investigated, all of them corresponding to specific resonant frequencies which are machine dependent. The lower the frequency, the deeper the investigation underneath the surface. A typical spectrum of Scanning Microwave Microscopy is shown as an example on Figure 2 with its resonant frequencies denoted by asterisks.

Last but not least, it is commonly acknowledged that stress variation inside a material will lead to a variation in amplitude of the microwave signal [12, 13]. In brief, this is exactly the ordinate variation of the asterisks that are studied in this paper.

In practice, measurements were carried out from 0.5 GHz to 13 GHz, which means that the waves go from the surface coating (13 GHz) down to the substrate (0.8 GHz). The temperature was kept between 22.3°C to 24°C and the air humidity between 25 % to 27 %.

2.3. RAMAN MICRO-SPECTROSCOPY

The Raman micro-spectroscopy examinations were performed with a XploRA PLUS from Horiba which was calibrated with a (111) Si single crystal. Measurements were performed using the parameters listed in Table 2. The diameter of the irradiating laser spot is about 0.87 μm and depth penetration is about 0.380 μm. Laser irradiance was kept under 1 GW as advised in previous works [14].

Parameters	Value
Acquisition time (s)	15
Accumulations	15
Objective	x50
Gratings	1800
Filter (%)	10

TABLE 2. Raman spectroscopy parameters

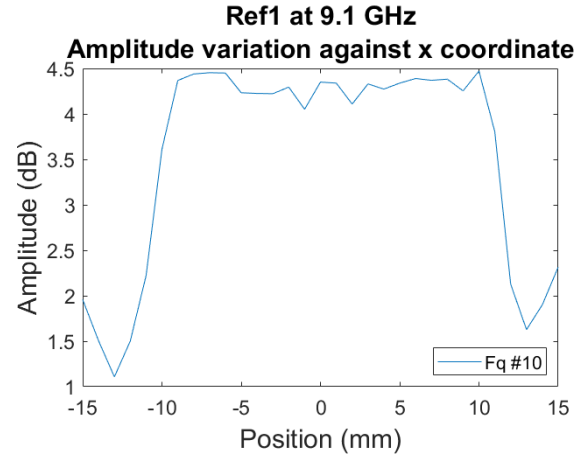This paper focuses on the shift of the most intense mode 555 cm^{-1} A_{1g} vibration [15, 16] as it is recog-

nized to produce a large change in the effective mode volume, thus undergoing the largest stress-induced frequency shifts [17]. The peak was fitted using either the pseudo-Voigt or the Lorentzian curve model based on the variation of the cumulative residuals. Iterative Curve Fitting (ICF) was performed under Origin2016.

2.4. X-RAY DIFFRACTION

Measurements were performed with a D8 Discover from Bruker equipped with a Cu source, in ψ (or χ) type assembly configuration and θ-2θ set up.

The post treatment was carried out with commercial software Leptos using the sin^2 ψ method. We focused on the shift of the peak at 125° with a peak evaluation chosen as standard and a stress model defined as normal in the software.

3. RESULTS AND DISCUSSION

3.1. X-RAY DIFFRACTION RESULTS

At first, XRD measurements highlighted that there were very low amounts of stress at the surface of both samples, although the one coated at high temperature seems to be in a slightly more compressive state as shown in Table 3:

Sample	Stress value (MPa)	Measurement Uncertainty (MPa)
Ref1	5.0	± 10.9
HT2	-52.4	± 4.5

TABLE 3. X-Ray Diffraction results

4. SCANNING MICROWAVE MICROSCOPY RESULTS

4.1. STRESS VARIATION OVER CENTERLINES

An exploration along the centerline involving about thirty measurements was performed on both samples.
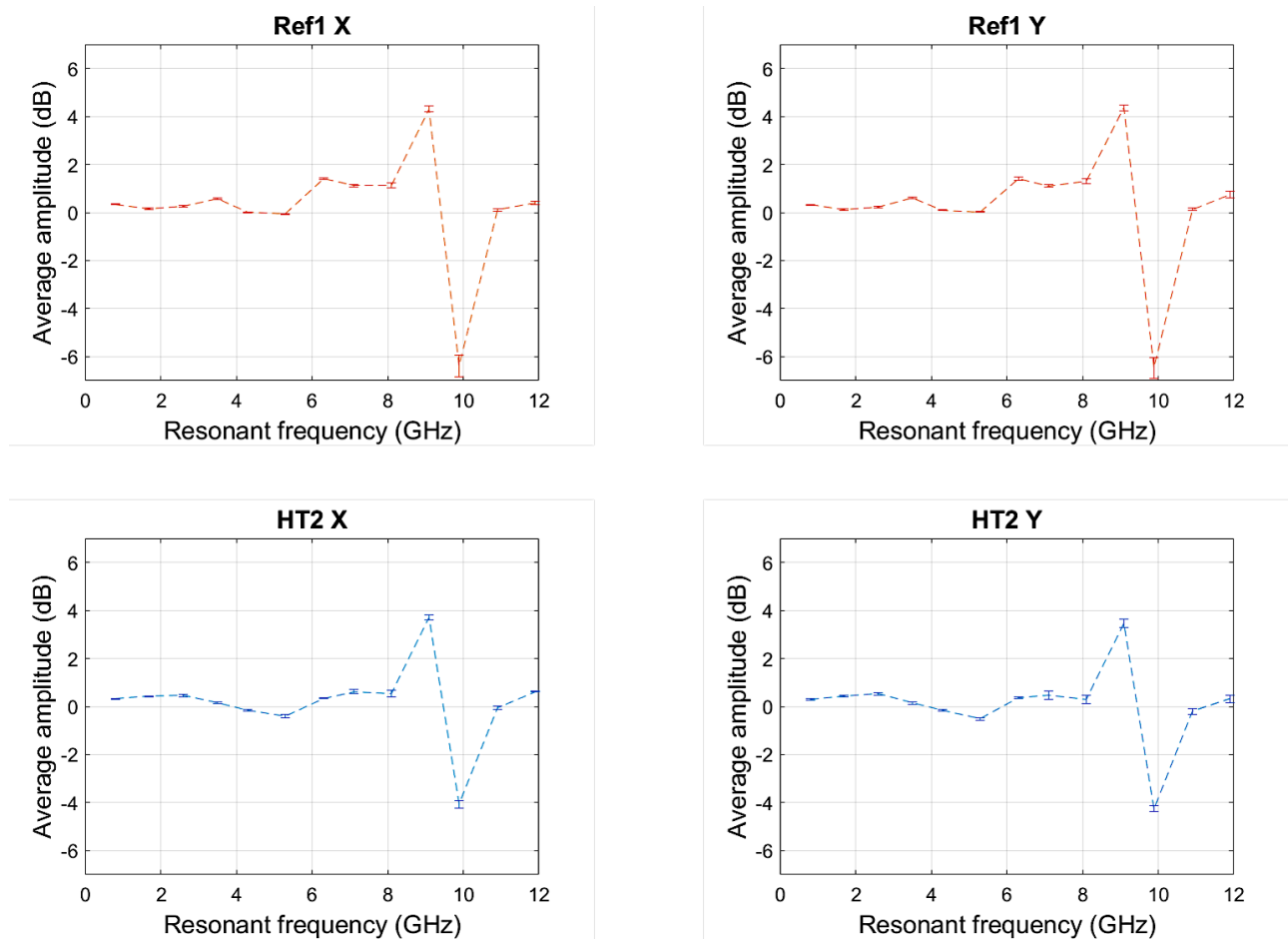
FIGURE 4. Averaged amplitude of SMM signal against frequency

Results show that edge effects like the one visible on Figure 3 at 9.1 GHz are likely to be found between 7.1 GHz and 10.9 GHz.

Change in solidification process may indeed occur near the edges of the sample as the number of degrees of freedom increases. This phenomenon is also to be considered when investigating closer to the very last sprayed layer where solidification was left to happen freely at ambient temperature. Steel substrate is likely to exhibit edge effects too regarding cutting and drilling processes it underwent.

In order to compare the state of stress at different depths between the two samples in a sound and relevant manner, only data between -5 mm to +5 mm were considered for the in-depth stress study.

5. In-depth stress variation

We computed the average amplitude value obtained for each frequency within the delimited area. We therefore plotted the average stress value against the working frequency which reflects the investigation depth in the material. Results are shown in Figure 4:

One can easily notice that both samples can be considered isotropic as levels of amplitude variate the same along the two directions. This result is consistent with what is expected from APS.

Moreover, the four curves exhibit the same steadily stress level as we investigate the [8-0.8] GHz range. Such a tendency leads to think that this reflected signal characterizes the substrate, which is consistent with results from deep hole drilling investigation on thermally sprayed ceramics [2]. Around the 9 GHz region would be the interface, whereas the 11.9 GHz to 10.9 GHz characterize the stress level within chromium oxides. Collecting such few data in the coating can be explained by the evanescent behavior of microwave within ceramics. In concrete terms, the wave train easily penetrates the material following an exponential law of propagation as mentioned in literature [18]. This could also explain that, despite the thickness difference between Ref1 and HT2, we collected the same amount of data in the two coatings. The authors want to set clear that SMM resonant frequencies are very unlikely to match with the same depth of investigation between the two samples.

6. Raman spectroscopy results

6.1. Stress variations over centerlines

Centerlines stress measurements were performed with Raman spectrometer to be compared to highest frequency (11.9 GHz) SMM results. The resulting raw Raman data are shown in dashed line on Figure 5.
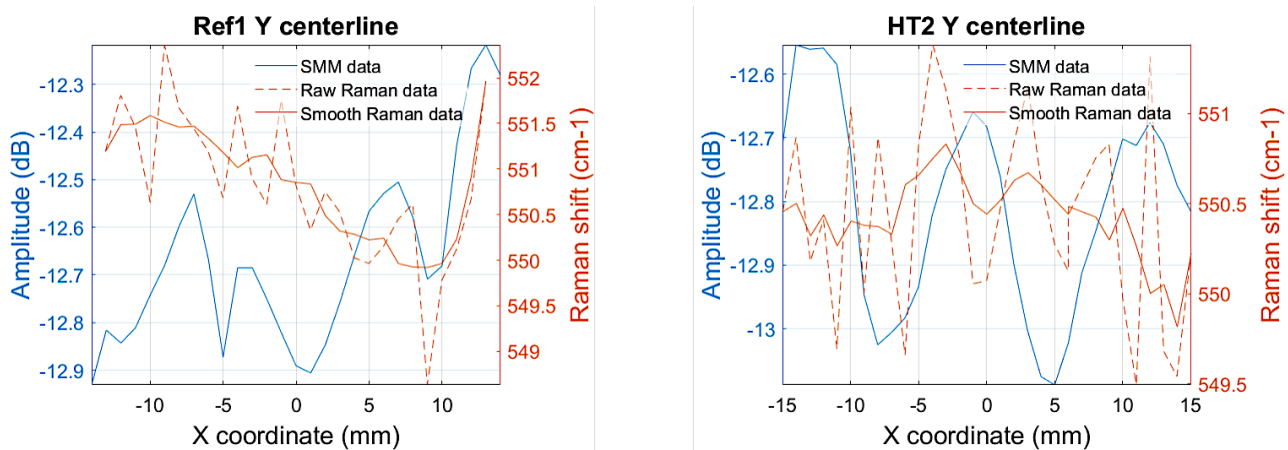
FIGURE 5. Correlation of stress measurements along Y centerlines for the two samples

To highlight clearer tendencies from them, a 5-points smoothing was applied, which does not impact curve extremities. From HT2 Y, Raman data reveal a strong wavy curve - especially in the 6 millimeters area from either side of the center - which is also exhibited by SMM results. Regarding Ref1 Y, raw Raman data oscillate around 551.25 cm^{-1} from -12 mm to 0 mm, while SMM data does around -12.75 dB. Then, as Raman data decrease down to 548.5 cm^{-1}, SMM ones increase up to -12.3 dB. At the last extremity of the curve, Raman data drastically increase whereas SMM ones start to decrease.

Although in practice stage position between the two instruments cannot perfectly match, resulting stress curves exhibit strong tendencies to face each other like mirror images.

As the zero-stress reference could not have been reliably determined yet, authors find it too hasty to establish the borderline between compressive and tensile stresses in this paper.

7. CONCLUSIONS

The present work establishes that SMM and Raman spectrometer reveal similar stress tendencies at the center of thermally sprayed ceramic coatings. The difference between the volume investigated by each two instruments may explain the dissimilar results closer to the edge. As the SMM showed consistent results regarding both top surface and in-depth investigations, a further study will assess microwave propagation law within Cr_2O_3.

REFERENCES

[1] T. W. Clyne, S. C. Gill. Residual stresses in thermal spray coatings and their effect on interfacial adhesion: A review of recent work. *Journal of Thermal Spray Technology* **5**(4):401–418, 1996. DOI:10.1007/bf02645271.

[2] G. Montay, A. Cherouat, J. Lu. Residual stress analysis in crankshaft using the hole drilling method. In *Materials Science Forum*, pp. 537–542. Trans Tech Publications Ltd., 2006. DOI:10.4028/0-87849-414-6.537.

[3] P. Withers, H. Bhadeshia. Residual stress. part 2 – nature and origins. *Materials Science and Technology* **17**(4):366–375, 2001. DOI:10.1179/026708301101510087.

[4] S. Kuroda, T. Fukushima, S. Kitahara. Significance of quenching stress in the cohesion and adhesion of thermally sprayed coatings. *Journal of Thermal Spray Technology* **1**(4):325–332, 1992. DOI:10.1007/bf02647160.

[5] S. Kuroda, T. Clyne. The quenching stress in thermally sprayed coatings. *Thin Solid Films* **200**(1):49–66, 1991. DOI:10.1016/0040-6090(91)90029-w.

[6] S. Kuroda, T. Clyne. The origin and quantification of the quenching stress associated with splat cooling during spray deposition. In *2nd Plasma Technik Symposium, Plasma Technik*, vol. 3, pp. 273–284. 1991.

[7] L. Pawlowski. *The Science and Engineering of Thermal Spray Coatings*. John Wiley & Sons, Ltd, 2008. DOI:10.1002/9780470754085.

[8] S. Kuroda. Properties and characterization of thermal sprayed coatings-a review of recent research progress. In *Thermal Spray Meeting the Challenges of the 21st Century, Proc. 15th Int. Thermal Spray Conf. May, 1998, Nice*, pp. 539–550. 1998.

[9] P. Withers, H. Bhadeshia. Residual stress. part 1 – measurement techniques. *Materials Science and Technology* **17**(4):355–365, 2001. DOI:10.1179/026708301101509980.

[10] Handbook of measurement of residual stresses. *Choice Reviews Online* **34**(04):34–2182–34–2182, 1996. DOI:10.5860/choice.34-2182.

[11] J. Mougin, T. L. Bihan, G. Lucazeau. High-pressure study of cr2o3 obtained by high-temperature oxidation by x-ray diffraction and raman spectroscopy. *Journal of Physics and Chemistry of Solids* **62**(3):553–563, 2001. DOI:10.1016/s0022-3697(00)00215-8.

[12] J. Mougin, N. Rosman, G. Lucazeau, A. Galerie. In situ raman monitoring of chromium oxide scale growth for stress determination. *Journal of Raman Spectroscopy* **32**(9):739–744, 2001. DOI:10.1002/jrs.734.

[13] V. Optasanu, E. Bourillot, P. Vitry, et al. High-resolution characterization of the diffusion of light chemical elements in metallic components by scanning microwave microscopy. *Nanoscale* **6**(24):14932–14938, 2014. DOI:10.1039/c4nr04017a.

[14] E. N. Aybeke, S. Ployon, M. Brulé, et al. Nanoscale mapping of the physical surface properties of human buccal cells and changes induced by saliva. *Langmuir* **35**(39):12647–12655, 2019. DOI:10.1021/acs.langmuir.9b01979.

[15] I. R. Beattie, T. R. Gilson. The single-crystal raman spectra of nearly opaque materials. iron(III) oxide and chromium(III) oxide. *Journal of the Chemical Society*

A: Inorganic, Physical, Theoretical p. 980, 1970. DOI:10.1039/j19700000980.

[16] J. Birnie, C. Craggs, D. Gardiner, P. Graves. Ex situ and in situ determination of stress distributions in chromium oxide films by raman microscopy. *Corrosion Science* **33**(1):1–12, 1992. DOI:10.1016/0010-938x(92)90014-t.

[17] M. SAKA, Y. JU, D. LUO, H. ABÉ. A method for sizing small fatigue cracks in stainless steel using microwaves. *JSME International Journal Series A* **45**(4):573–578, 2002. DOI:10.1299/jsmea.45.573.

[18] R. Zoughi. *Microwave Non-Destructive Testing and Evaluation.* Springer Netherlands, 2000. DOI:10.1007/978-94-015-1303-6.